

## RBS and UV-VIS-NIR studies of low energy Mn<sup>+</sup> ion implanted in GaAs substrate

SHARAD TRIPATHI<sup>1,2</sup>, S K DUBEY<sup>2</sup>, V. S. UPADHYAY<sup>2</sup>

<sup>1</sup>Department of Physics, G. N. Khalsa College, Matunga, Mumbai, India.

<sup>2</sup>Department of Physics, University of Mumbai, Vidyanagari, Mumbai, India.  
e-mail: srdtripathi@gmail.com

### Abstract

*In this study, un-doped GaAs were uniformly implanted with 325 keV Mn<sup>+</sup> ions for the various fluences varying from  $1 \times 10^{15}$  to  $2 \times 10^{16}$  ions cm<sup>-2</sup> using 1.7 MV Tandatron accelerator at IGCAR, Kalpakkam. RBS technique was used for their characterization and was found to decrease in scattering yield between the channel numbers 650 to 750 with falling edge showed reduction in the volume concentration of the GaAs due to the presence of implanted manganese ions in the region. UV-VIS-NIR spectra of non-implanted and samples implanted for various fluences ranging from  $1 \times 10^{15}$  to  $2 \times 10^{16}$  ions cm<sup>-2</sup> were performed in the spectral region 150 nm to 3300 nm. The values of the absorption coefficient of Mn<sup>+</sup> ion implanted GaAs samples estimated from the transmission spectra were found to increase with ion fluence. The increase in absorbance with respect to ion fluence indicates the increase in defects and disorder in the ion implanted layers. The band gap energy of the samples implanted with the fluence of  $1 \times 10^{15}$ ,  $5 \times 10^{15}$ ,  $1 \times 10^{16}$  and  $2 \times 10^{16}$  ions cm<sup>-2</sup> estimated from the  $\alpha^2$  versus photon energy curve were found to be 1.370, 1.332, 1.323 and 1.309 eV respectively.*

**Keywords:** Ion Implantation, GaAs, Mn, RBS, UV.

### Introduction

Implantation techniques have been traditionally used to modify the physical properties of semiconducting materials, such as the free carrier concentration [1] or the n- or p-type semiconducting behavior [2]- More recently, ion implantation has been used to induce site-selective growth of semiconducting quantum dots for strong three dimensional carrier confinement [3]. This approach can overcome the low solubility of magnetic ions into III/V semiconductors, avoiding the formation of phase separation above a certain doping [4]. Nevertheless, the ion implantation originates lattice damage and creates a great variety of mobile and stable defects, known as implantation-induced defects. If implantation-induced defects such as Frenkel pairs (interstitials and vacants) are mobile at the implantation temperature, then a significant annihilation of the damage can occur during the implantation because of the dynamic annealing processes

[5, 6]. Moreover, additional and selective extermination of the implantation-induced defects can be achieved by annealing the specimens at a desired temperature after implantation [7]. The mechanism of the formation and annihilation of defects in implanted semiconductors notably influences their physical properties and, therefore, it is of great scientific and technological interest [8, 9]. These native defects can play an important role for the reconstruction of the lattice damage after the implantation. The characterization of the lattice disorder induced by the misfit dislocation at the InAs/GaAs inter-face has been already carried out by Williams et al. using Rutherford backscattering spectrometry in channeling geometry (RBS/ C) [10]. Actually, RBS/C has been revealed as a precise and useful tool for the study of crystal quality and strain of epitaxial layers in hetero-junctions or super-lattices [11, 12]. The crystal quality and lattice order of the epitaxial layers is described by the ratio of yields (number of backscattered atoms) measured in aligned and in random configuration, also called normalized yield ( $x$ ) Thus, a low  $x$  is a sign of good epitaxial quality (high order degree or crystalline feature), whether a high  $x$  would indicate a low epitaxial quality and/or lattice disorder. RBS/C is also a sensitive probe for strain, which can be measured by means of the angular displacement (known as kink angle) between the dips of the layer and the substrate along an oblique axis [13,14].

In the present work, we studied the structural and optical properties of gallium arsenide after implantation with 325 keV  $Mn^+$  ions with various fluences varying from  $1 \times 10^{15}$  to  $2 \times 10^{16}$  ions  $cm^{-2}$  using Rutherford Backscattering Spectrometry and UV-Vis -IR techniques.

### Experiment details

In this study, un-doped gallium arsenide samples were implanted with 325 keV  $Mn^+$  ions for the fluences of  $1 \times 10^{15}$ ,  $5 \times 10^{15}$ ,  $1 \times 10^{16}$  and  $2 \times 10^{16}$  ions  $cm^{-2}$  using 1.7 MV Tandatron accelerators at IGCAR, Kalpakkam. The implantation energy of 325 keV was selected on the basis of the SRIM code calculations [14]. Projected range ( $R_p$ ) and standard deviation ( $\Delta R_p$ ) of the 325 keV  $Mn^+$  ions in gallium arsenide were found to be 155.6 nm and 66.7 nm respectively. Rutherford Backscattering Spectrometry measurement was also performed at IGCAR, Kalpakkam using same Accelerators. The helium gas is bled into a source bottle through a fine metering valve and RF field was applied to two electrodes on the outside of the source bottle. A well collimated beam of 2 MeV helium ion was incident normal to the surface of the implanted sample and backscattered ions were detected at 170 degree. Typical beam current and collected charges were 10nA and 10 $\mu$ C respectively and UV-VIS-NIR transmission spectra were performed on UV-VIS-NIR spectrometer (Shimadzu UV-3600) in wavelength regions 150 nm to 3300 nm have been used to investigate optical properties of  $Mn^+$  ion implanted samples.

## Results and Discussion

### Rutherford Backscattering Spectrometry Study

Figure 1 shows the RBS spectra of the GaAs samples implanted with 325 keV Mn<sup>+</sup> at fluences of 1 x 10<sup>15</sup>, 5 x 10<sup>15</sup>, 1 x 10<sup>16</sup>, and 2 x 10<sup>16</sup> ions cm<sup>-2</sup> at room temperature. The decrease in scattering yield between the channel numbers 650 to 750 with falling edge showed reduction in the volume concentration of the GaAs due to the presence of implanted manganese ions in the region. The total manganese implantation fluence and concentration at projected range (Rp) are estimated from the RBS using the following relation [11-13];

$$Y = \frac{Q \cdot \Omega \cdot N \cdot \sigma}{\cos \theta}$$

where, Y is the surface yield of the sample film (in counts / channel), QΩ is charge x solid angle product (sr), σ is the differential cross section for the ion of the given energy into the detector ( cm<sup>2</sup>/ sr), θ is the beam incidence angle from the normal and N is the concentration ( cm<sup>-3</sup>). The values of implanted fluence and concentration at R<sub>p</sub> are given in Table -1. The slight variation in the calculated and experimental values may be due to sputtering of the implanted ions and radiation enhanced diffusion. The distribution of manganese in gallium arsenide is of Gaussian shape with a peak at depth of 169.7 nm. The projected range (Rp) and longitudinal straggling (ΔRp) estimated from the RBS measurement were found to be 169.7 nm and 71.3 nm respectively. These values are found to be in good agreement with the projected range (155.6 nm) and longitudinal straggling (71.3 nm), calculated for 325 keV Mn<sup>+</sup> in GaAs using SRIM code. Figure 2 shows the RBS depth profile of manganese ion implanted samples along with the theoretical depth profile. The experimental and theoretical profiles were found to match closely. However, the shape of the depth profile from the RBS measurement were found to be broader than that of the theoretical calculated values due to diffusion of manganese atoms.

**Table -1**

Total manganese fluence and concentration were estimated from RBS data for the implanted samples.

Fluence (ions cm <sup>-2</sup> )		Concentration ( x 10 <sup>22</sup> cm <sup>-3</sup> )	
Implanted	Measured from RBS	Calculated from the implantation fluence	Estimated from RBS
1 × 10 <sup>15</sup>	1.01 × 10 <sup>15</sup>	0.1035	0.1030
5 × 10 <sup>15</sup>	4.44 × 10 <sup>15</sup>	0.0529	0.0526
1 × 10 <sup>16</sup>	0.88 × 10 <sup>16</sup>	0.0265	0.0261
2 × 10 <sup>16</sup>	1.78 × 10 <sup>16</sup>	0.0057	0.0057

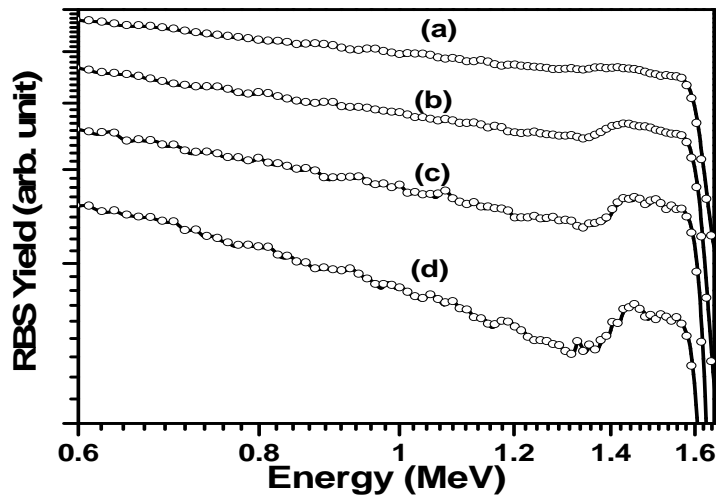


**Figure 1:** RBS spectra (yield versus channel number) of GaAs samples implanted with at 325 keV  $Mn^+$  at fluence of (a)  $1 \times 10^{15}$ , (b)  $5 \times 10^{15}$ , (c)  $1 \times 10^{16}$  and (d)  $2 \times 10^{16}$  ion  $cm^{-2}$ .

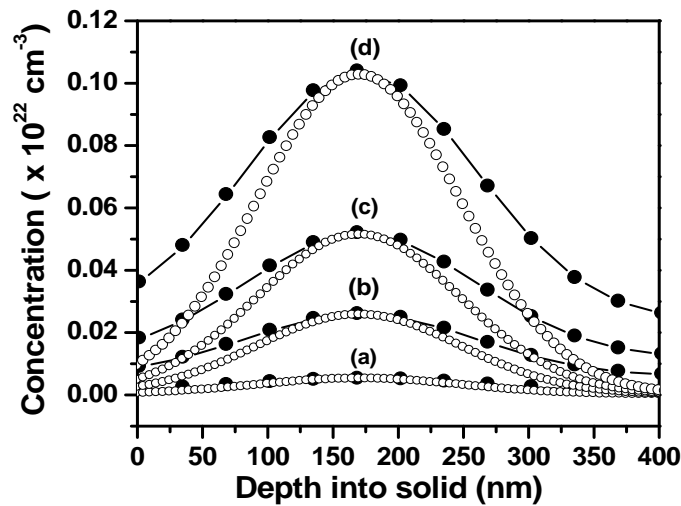


**Figure 2:** Comparison of theoretical and experimental manganese concentration depth profiles of GaAs samples implanted at 325 keV with  $Mn^+$  at fluences of (a)  $1 \times 10^{15}$ , (b)  $5 \times 10^{15}$  (c)  $1 \times 10^{16}$  and (d)  $2 \times 10^{16}$  ion  $cm^{-2}$  (●-Experimental, ○-Theoretical).

### Ultra-Violet Visible (UV-VIS) NIR Study

UV-VIS-NIR studies were performed on non-implanted and the samples implanted for the fluences of  $1 \times 10^{15}$ ,  $5 \times 10^{15}$ ,  $1 \times 10^{16}$  and  $2 \times 10^{16}$  ions  $cm^{-2}$ . Absorbance spectra of the samples implanted with 325 keV  $Mn^+$  ions in range fluence between  $1 \times 10^{15}$  to  $2 \times 10^{16}$   $cm^{-2}$  are shown in Figure 3. The values of absorbance of the  $Mn^+$  ion implanted samples were found to be increased with respect to ion fluence. For direct band gap materials like GaAs, momentum conserving transitions between parabolic bands and

absorption coefficient increases with the square root of photon energy. In order to estimate the optical band gap  $\alpha^2$  versus photon energy curve were plotted. The non-implanted GaAs shows a band gap of 1.393 eV while the band gap energy of the samples implanted at the fluence of  $1 \times 10^{15}$ ,  $5 \times 10^{15}$ ,  $1 \times 10^{16}$  and  $2 \times 10^{16}$  ions  $\text{cm}^{-2}$  were found to be a shift in band gap. This shift in band gap is possible due to the strain induced in GaAs lattice due to Mn ion incorporation.

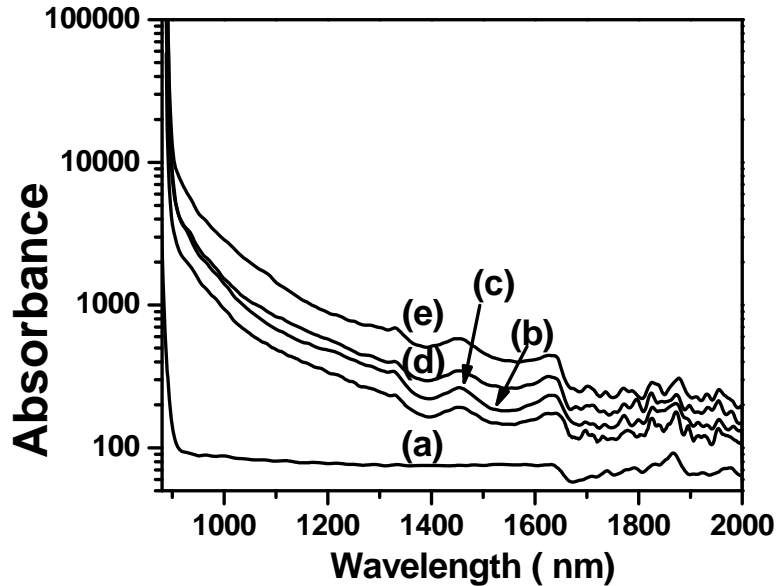


**Figure 3:** Absorbance spectra of gallium arsenide; (a) non-implanted and implanted with 325 keV  $\text{Mn}^+$  ions at fluence of (b)  $1 \times 10^{15}$ , (c)  $5 \times 10^{15}$ , (d)  $1 \times 10^{16}$  and (e)  $2 \times 10^{16}$  ions  $\text{cm}^{-2}$ .

The optical density ( $\alpha \cdot d$ ) was calculated from the measured spectra by using the following expression taking into account the multiple reflections;

$$\frac{I}{I_0} = \frac{(1-R)^2 e^{-\alpha d}}{1-R^2 e^{-2\alpha d}}$$

where  $I_0$  and  $I$  are incident and transmitted intensities respectively,  $d$  ( $= 350 \mu\text{m}$ ) is the thickness of the sample. The reflectivity ( $R$ ) of gallium arsenide was estimated using the following expression;

$$R = \frac{(n-1)^2 + k^2}{(n+1)^2 + k^2},$$

where  $n$  ( $= 3.3$ ) is the refractive index and  $k = \lambda \alpha / 4\pi$  is the propagation constant. The value of  $R$  determined using the above equation was found to be 0.34 and assumed to be constant over the entire photon energy range. Figure 4 shows the optical density ( $\alpha \cdot d$ ) versus photon energy curves for both non-implanted and samples implanted for the fluence of  $1 \times 10^{15}$ ,  $5 \times 10^{15}$ ,  $1 \times 10^{16}$  and  $2 \times 10^{16}$  ions  $\text{cm}^{-2}$ .

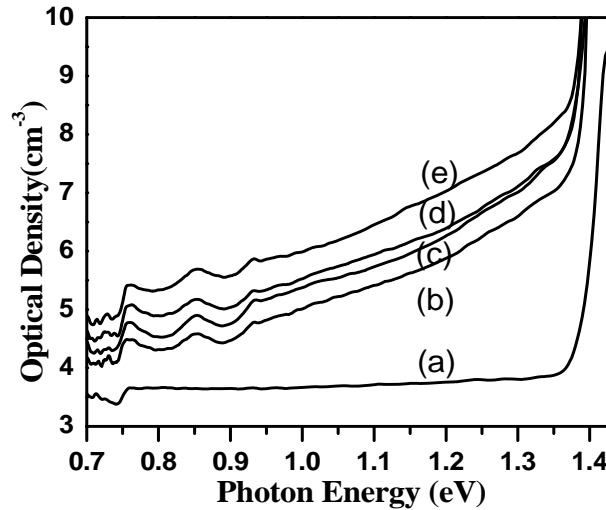


**Figure 4:** Optical density vs photon energy curves of GaAs; (a) non-implanted and samples implanted with 325 keV Mn<sup>+</sup> ions at fluence of (b) 1 × 10<sup>15</sup>, (c) 5 × 10<sup>15</sup>, (d) 1 × 10<sup>16</sup> and (e) 2 × 10<sup>16</sup> ions cm<sup>-2</sup>.

The increase in the optical density with ion fluence (Figure 4) indicates the increase in the defects and disorder in the implanted layer. The defect-densities in the implanted samples were estimated from the following relation;

$$N_s = \left[ \frac{m_e c \epsilon}{2\pi h e^2} \right] \left[ \frac{\mu(1-2\mu^2)^2}{18\mu^4 f} \right] \int \alpha(\text{excess}) dE$$

where  $\int \alpha(\text{excess}) dE$  is the difference in the areas of non-implanted and samples implanted with different ion fluence extracted from Figure 4,  $\mu$  is the refractive index,  $c$  is the speed of light,  $e$  is the electronic charge and  $f$  is the oscillator strength and has been assumed to be one. In this calculation, the density of defects in the samples implanted with ion fluences of 1 × 10<sup>15</sup>, 5 × 10<sup>15</sup>, 1 × 10<sup>16</sup> and 2 × 10<sup>16</sup> ion cm<sup>-2</sup> were found to be 1.27 × 10<sup>16</sup>, 1.51 × 10<sup>16</sup>, 1.82 × 10<sup>16</sup> and 2.38 × 10<sup>16</sup> cm<sup>-3</sup> respectively.

## Conclusions

The 325 keV Mn<sup>+</sup> ion implantation in semi-insulating GaAs was carried out with various fluences. The RBS spectra of GaAs samples implanted with various fluences showed decrease in scattering yield with ion fluence. These results showed the reduction in the volume concentration of the GaAs due to the presence of implanted Mn<sup>+</sup> ions. UV-VIS-NIR studies revealed the increase in the absorption with increase in ion fluence.

## Acknowledgments

The authors are thankful to G. N. Khalsa College, Matunga, Mumbai and Maharashtra for providing the financial support and others.

## References

1. Don H. Lee, W. James Mayer, Proceedings of the *IEEE* 62 (1974) 1214.
2. K.Y. Wang, K.W. Edmonds, R. P. Campion et al, *J. Appl. Phys.* 95, (2004) 6512.
3. M. Mehta, D. Reuter, A. Melnikov, A.D. Wieck, *Appl. Phys. Lett.* 91 (2007) 123108.
4. L. J. Hu, Y. H. Chen, X. L. Ye, Y. H. Jiao, L.W. Shi, Z. G. Wang, *Physica E: Low-dimensional Systems and Nanostructures* 40 (2008) 2869.
5. S. Tripathi, R. L. Dubey, S. K. Dubey, A. D. Yadav, P. Kumar and D. Kanjilal, *American Institute of Physics* 1313 (2010) 100.
6. J. Shi, J. M. Kikkwa, D. D. Awschalom, G. Medeiros-Ribeiro, P. M. Petroff, K. Babcock, *J. Appl. Phys.* 79 (1996) 5296.
7. R. González-Arrabal, Y. González, L. González, M. García-Hernández, F. Munnik, M.S. Martín-González, *J. Appl. Phys.* 105 (2009) 073911.
8. S. Tripathi, S. K. Dubey, A. D. Yadav et al, *DAE SS P Symposium* 54 (2009) 1064.
9. S. Tripathi, S. K. Dubey, A. D. Yadav and D. C. Kothari, B. K. Panigrahi and K. G. M. Nair, *American Institute of Physics* 1276 (2009) 344.
10. H. Munekata, H. Ohno, S. von Molnar, S. von Molnar, Armin Segmüller, LL Chang, L. Esaki, *Phys. Rev. Lett.* 63 (1989) 1849.
11. W. K. Chu, J. W. Mayer, M. A. Nicolet, *Backscattering Spectroscopy*, Academic press, New York, 1978.
12. O. Usova, D. Koleske, K.E. Sickafus, *Nucl. Instr. Meth. B* 267 (2009) 2962.
13. J. W. Mayer, *Electron Devices Meeting, 1973 International*, (1973) 3.
14. J. F. Ziegler, M.D. Ziegler, J. P. Biersack, SRIM-2008

KKKK